

Peter BUDAY ¹⁾
Jakub ČURPEK ^{1,2)}

¹⁾ Slovak University of Technology
in Bratislava, Faculty of Civil
Engineering

^{1,2)} Brno University of Technology,
Faculty of Civil Engineering

Double-skin Facade Configuration to Increase its Thermal Efficiency: Simulation Study



Konfigurácia dvojitej fasády pre zvýšenie jej tepelnej účinnosti: energetická simulačná štúdia

Nowadays, double-skin facades represent a distinctive architectural element in modern buildings. However, their real thermal impact on the overall building energy performance can be enhanced by the facades internal modifications. The main modifications include the dimensions of the facade cavity, the intensity of the solar radiation, the combination of the optical parameters of both the transparent and opaque parts, as well as the possibility to have a natural or forced air flow movement in the cavity. The presented paper is focused on the quantification of the different levels of the above-mentioned factors as the boundary conditions for the thermal performance of the air flow movement in the facade cavity through its overall height.

Keywords: double-skin facade, energy performance, CFD simulation

Dvojplášťové fasády tvoria v súčasnosti na moderných stavbách zaujímavý a výrazný architektonický prvok. Ďaleko väčší prínos ale tvorí ich reálny účinok na celkovú energetickú bilanciu budovy, ako aj vytvorenie tepelnej pohody v nej. Tento prínos do značnej miery ovplyvňuje niekoľko významných faktorov. Medzi tie najhlavnejšie patrí konštrukčná šírka tohto medzipriestoru, intenzita slnečného žiarenia, kombinácia optických parametrov oboch jej transparentných častí (vnútornej a vonkajšej), ako aj možnosť jeho prirodzeného či technikou podporeného odvetrávania. Práve posledne zmieňovaný faktor, v kombinácii so spôsobom odvetrávania a aplikáciou niekoľkých netransparentných častí, výrazne ovplyvňuje okrajovú podmienku teplovýmenného obalu budovy a tak do značnej miery ovplyvňuje aj energetickú bilanciu budovy. A práve kvantifikácia toho tvorí podstatnú časť, náplň predkladaného príspevku.

Klíčovú slova: dvojplášťová fasáda, energetická bilancia, CFD simulácia

INTRODUCTION

The presented paper can be divided into two main parts. In the first part, the study of the influence of several boundary conditions on the performance of the double-skin facade (DSF) with a forced air movement in the upper part of the facade cavity (heat pump implementation) together with a reduced flow can be found. In the second part, the natural air flow movement in the facade cavity was investigated.

THEORY OF DOUBLE-SKIN FACADES

Double-skin facades, as a modern architectural element, still receive considerable attention in the scientific community. The generalisation of their impacts on the building energy saving potential has revealed the main advantages (with consideration to the technical design aspects) in symbiosis with the results achieved in real buildings [1]. Its thermal performance represents a significant factor influencing a facade's selection and application in real buildings. The computational methods of the DSF performance prediction are often based on different principles, one of which is the so-called "response factor" of the external boundary condition, towards this facade [2]. Many parametric studies have been carried out investigating the physical phenomena in DSFs, which took the whole set of variables that affected the results of energy savings into account [3]. A current trend is especially seen in the application of DSFs on high-rise buildings, where some of the important factors may be its height position and localisation. Moreover, existing buildings can be suitably supplemented by incorporating an innovative element of DSF in the process of their reconstruction [4]. The DSF can be realised with the support of building services technology, but also as a natural system

based on the basic physical principles of air flow [5-6]. A separate chapter of research and development of DSFs is regarding the application of blinds in the facade cavity, which can also significantly affect the energy effect of the entire facade [7], as well as the direct dependence of the air flow on the cavity width [8].

SIMULATION MODEL

For the present study, a CFD 3D model of a DSF was created with a total (visible) length of 4500 mm, varied facade cavity widths (600 to 1500 mm) and a height of four floors having a construction floor height of about 3450 mm.

The outer glazing is simple (with parameters $R_{E1} = 6 \%$, $A_{E1} = 34 \%$, $T_{E1} = 60 \%$ a $U_{g1} = 4,60 \text{ W}/(\text{m}^2\cdot\text{K})$) and the inner glazing is insulating triple glazing (with parameters $R_{E2} = 33 \%$, $A_{E2} = 20 \%$, $T_{E2} = 47 \%$ and $U_{g2} = 0,60 \text{ W}/(\text{m}^2\cdot\text{K})$).

The remaining non-transparent structures were modelled in accordance with the current standard requirements of the thermal protection of buildings [9], the wall structure – a reinforced concrete wall (250 mm) and mineral wool (180 mm), $U_{\text{wall}} = 0.205 \text{ W}/(\text{m}^2\cdot\text{K})$ and a flat roof – a reinforced concrete slab (180 mm), a sloping lightweight concrete layer (100 mm) and mineral wool (220 mm) $U_{\text{roof}} = 0.150 \text{ W}/(\text{m}^2\cdot\text{K})$.

The inlet opening of the DSF is in the lower part, with an area identical to the floor area of the facade cavity (the effective area of the cover grille is 70%) and in the upper part is located in an opening intended for the forced and natural outlet.

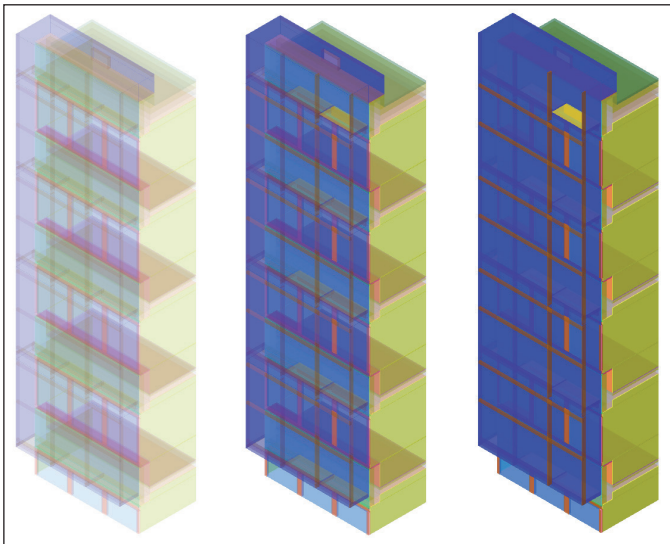


Figure 1 CFD model of the investigated DSF

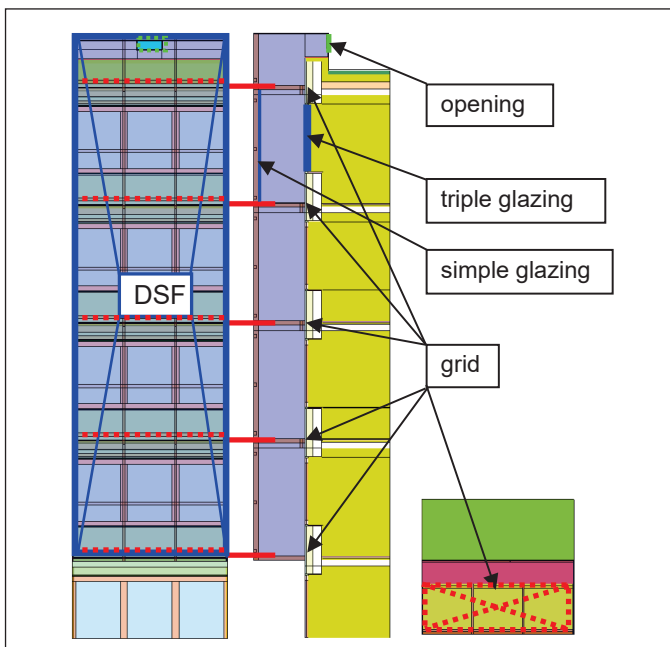


Figure 2 CFD model of the investigated DSF

At the level of each ceiling, a walkable full-area grid is modelled at the floor level, with a total effective area of 70%. The 3D simulation model itself is depicted in Fig. 1 and Fig. 2.

All the case simulations were realised in the calculation program FLOVENT [10], at the boundary condition of the outside air temperature of $-11.0\text{ }^{\circ}\text{C}$, without considering the effect of wind.

The building's simulation model has the overall dimensions of $4.5 \times 4.0 \times 17.7\text{ m}$. Due to the modelling of the parameters of the free air flow movement in its surrounding area, it was further widened by 2.0 m in front of the facade (also due to the variant extension of the double-skin facade) and by 1.5 m above the highest level of the attic.

The computational network is modelled using the internal tool of the network creation program, with thickening even in the surrounding area of all surfaces, as well as a sufficient number of cells in the individual modelled elements, especially the glazing. The optimal design of the network leads to the convergence of the solution in the range of 500 –

1000 computational iterations (depending on the specific variant of the model). The total number of computational cells of the model is in the range of 2.08 to 2.83 million cells, increasing in dependency to the width of the facade cavity.

The convergence of the solution itself was controlled by means of control points, which were located in the exposed part of the model and, thus, directly in the double-skin facade, evenly along its entire height.

The program-integrated turbulence model KVEL K-Epsilon was used to calculate the turbulence.

The solar radiation was modelled using an integrated solar configurator with intensities of $200 - 1000\text{ W/m}^2$, always in a position perpendicular to the facade, at a constant height angle, the impact of the sunlight on the facade is 45° .

SIMULATION STUDY – MECHANICAL VENTILATION

The primary assumption was, in addition to the positive effect of the increased air temperature of the facade cavity (as a boundary condition of the interior spaces in the winter), the use of the energy from the facade cavity as a direct input to the heat pump. The air flow in this location was considered at the levels of 2000, 4000 and 6000 m^3/h (expressed in the physical unit m^3/s in the tables and graphs, i.e., the values of 0.555, 1.111 and 1.666).

The second variable in the parametric study was the intensity of the incident solar radiation at four basic levels of 200, 400, 600 and 800 W/m^2 .

The last variable in the energy simulation was the width of the facade cavity, gradually modelled with dimensions of 600, 900, 1200 and 1500 mm.

OUTPUTS – MECHANICAL VENTILATION

The results of the simulations are presented in Table 1, which presents the average air temperatures in the facade cavity of the DSF, in dependence on the different air flow, the width of the cavity and the intensity of the incident solar radiation, the graphical representation is depicted in Fig. 3.

Table 2 shows the instantaneous energy output of the DSF - calculated by the air flow movement at the exhaust level, in combination with the average air temperature at the exhaust. Fig. 4 documents this quantity graphically.

In accordance with presented results, the width of the facade cavity itself only has a minimal effect on the air temperature.

However, the intensity of the incident solar radiation has a much greater influence, which ranges from 200 to 800 W/m^2 in the simulation and increases the average air temperature in the facade cavity by up to about 8.0 K (with the smallest air flow at the outlet of 2000 m^3/h). However, this increase is considerably reduced at the highest modelled flow rate of 6000 m^3/h to about half (3.5 K).

By transforming the air flow and air temperature at the exhaust, it is then possible to subsequently identify the so-called “Energy performance of a DSF”, where it is also possible to observe the minimal effect of the facade cavity's width on this quantity.

As the intensity of the solar radiation quadruples (from 200 to 800 W/m^2), this output increases almost identically as well. On the contrary,

a threefold increase in the air flow at the exhaust level (from 2000 to 6000 m³/h) only brings about a 1.4 - 1.5-times increase in the energy output of the facade.

Table 1 Average air temperature in the facade cavity

| variant | air flow | | |
|--------------------------------|-------------------------|-------------------------|-------------------------|
| | 0.555 m ³ /s | 1.111 m ³ /s | 1.666 m ³ /s |
| 600 mm + 200 W/m ² | -8.14 | -9.18 | -9.56 |
| 600 mm + 400 W/m ² | -5.69 | -7.72 | -8.40 |
| 600 mm + 600 W/m ² | -3.18 | -6.25 | -7.24 |
| 600 mm + 800 W/m ² | -0.66 | -4.76 | -6.08 |
| 900 mm + 200 W/m ² | -8.08 | -9.31 | -9.65 |
| 900 mm + 400 W/m ² | -5.51 | -7.88 | -8.61 |
| 900 mm + 600 W/m ² | -2.87 | -6.35 | -7.60 |
| 900 mm + 800 W/m ² | -0.17 | -4.81 | -6.57 |
| 1200 mm + 200 W/m ² | -8.06 | -9.34 | -9.75 |
| 1200 mm + 400 W/m ² | -5.46 | -7.85 | -8.83 |
| 1200 mm + 600 W/m ² | -2.73 | -6.32 | -7.76 |
| 1200 mm + 800 W/m ² | 0.04 | -4.77 | -6.62 |
| 1500 mm + 200 W/m ² | -8.11 | -9.33 | -9.85 |
| 1500 mm + 400 W/m ² | -5.65 | -7.88 | -8.82 |
| 1500 mm + 600 W/m ² | -3.14 | -6.39 | -7.72 |
| 1500 mm + 800 W/m ² | -0.54 | -4.88 | -6.61 |

Table 2 Immediate facade performance (kW)

| variant | air flow | | |
|--------------------------------|-------------------------|-------------------------|-------------------------|
| | 0.555 m ³ /s | 1.111 m ³ /s | 1.666 m ³ /s |
| 600 mm + 200 W/m ² | 3.88 | 4.94 | 5.68 |
| 600 mm + 400 W/m ² | 7.03 | 8.91 | 10.25 |
| 600 mm + 600 W/m ² | 10.18 | 12.85 | 14.76 |
| 600 mm + 800 W/m ² | 13.32 | 16.79 | 19.25 |
| 900 mm + 200 W/m ² | 3.99 | 4.90 | 5.55 |
| 900 mm + 400 W/m ² | 7.29 | 8.98 | 10.08 |
| 900 mm + 600 W/m ² | 10.60 | 13.09 | 14.65 |
| 900 mm + 800 W/m ² | 13.90 | 17.20 | 19.23 |
| 1200 mm + 200 W/m ² | 4.01 | 4.93 | 5.53 |
| 1200 mm + 400 W/m ² | 7.34 | 9.08 | 10.15 |
| 1200 mm + 600 W/m ² | 10.70 | 13.24 | 14.81 |
| 1200 mm + 800 W/m ² | 14.04 | 17.41 | 19.49 |
| 1500 mm + 200 W/m ² | 3.86 | 4.81 | 5.41 |
| 1500 mm + 400 W/m ² | 7.05 | 8.82 | 9.94 |
| 1500 mm + 600 W/m ² | 10.27 | 12.85 | 14.51 |
| 1500 mm + 800 W/m ² | 13.48 | 16.89 | 19.05 |

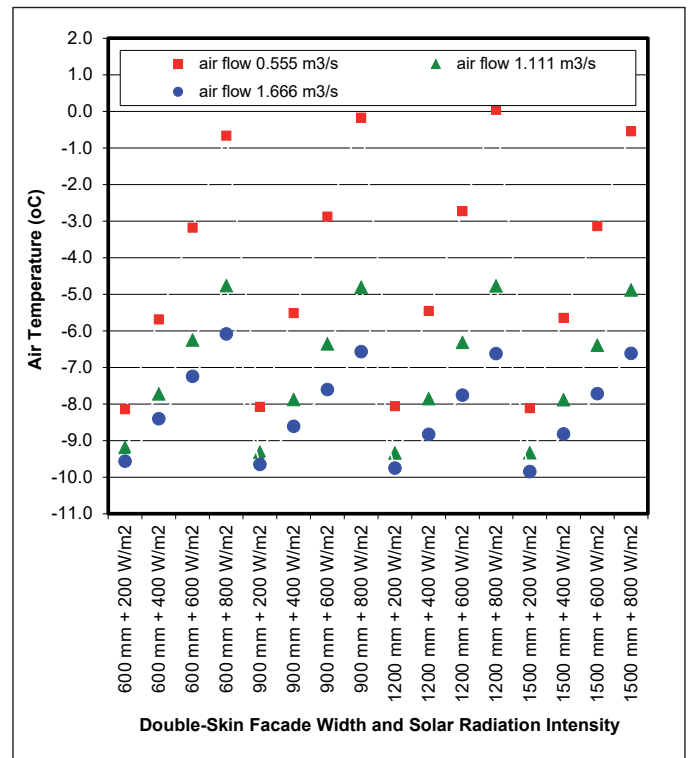


Figure 3 Average air temperature in the facade cavity

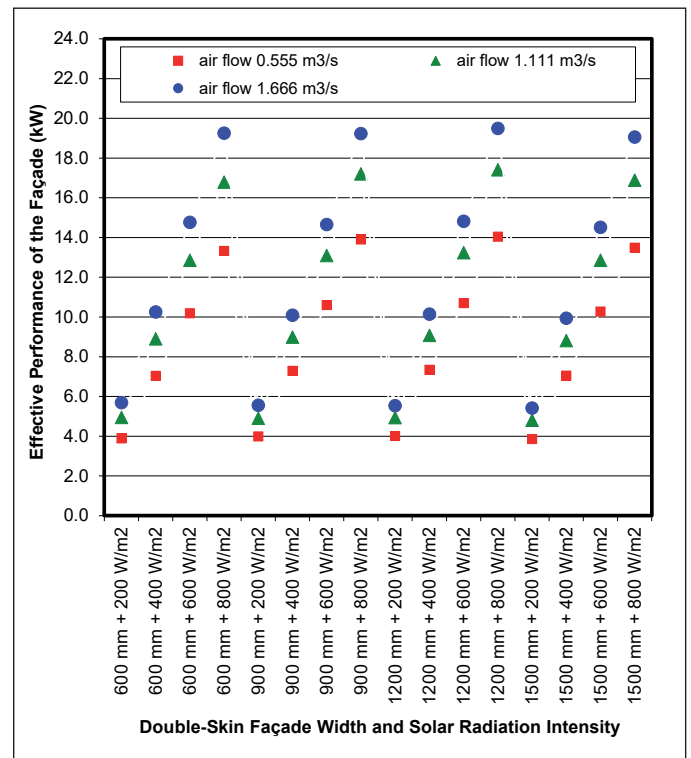


Figure 4 Immediate facade performance

SIMULATION STUDY – NATURAL VENTILATION

In this part, the forced ventilation of the air extraction was replaced by an effective area of the opening, which will work naturally, based on the physical principles of buoyancy-driven air flow, depending on the temperature. In the subsequent study, four variants were considered - the area of this opening was set up to 0.125, 0.250, 0.375 and 0.500 m². The intensity of the solar radiation was, in contrast to the previous part,

alternatively extended by the highest intensity of the solar radiation – 1000 W/m². As the width of the facade cavity in the previous part of the analysis did not show any significant effect, it was reduced to only two values - 600 and 1200 mm.

OUTPUTS – NATURAL VENTILATION

The results of the simulations are presented in Table 3, which presents the air temperatures at the outlet level from the cavity of the DSF, depending on the area of the opening (outlet), the width of the cavity as well as the intensity of the incident solar radiation for the cavity width of 600 mm (Fig. 5), and for a width of 1200 mm (Fig. 6).

Table 3 The air temperature at the exhaust

| No. | variant | 0600 mm | 1200 mm |
|-----|--|---------|---------|
| 01 | 200 W/m ² + 0.125 m ² | -10.80 | -10.83 |
| 02 | 400 W/m ² + 0.125 m ² | 11.27 | 14.62 |
| 03 | 600 W/m ² + 0.125 m ² | 16.28 | 19.28 |
| 04 | 800 W/m ² + 0.125 m ² | 21.63 | 22.71 |
| 05 | 1000 W/m ² + 0.125 m ² | 23.61 | 26.66 |
| 06 | 200 W/m ² + 0.250 m ² | -10.90 | -10.91 |
| 07 | 400 W/m ² + 0.250 m ² | 10.74 | -10.83 |
| 08 | 600 W/m ² + 0.250 m ² | 15.68 | 17.94 |
| 09 | 800 W/m ² + 0.250 m ² | 18.75 | 20.19 |
| 10 | 1000 W/m ² + 0.250 m ² | 19.59 | 22.66 |
| 11 | 200 W/m ² + 0.375 m ² | -10.93 | -10.94 |
| 12 | 400 W/m ² + 0.375 m ² | -10.83 | -10.87 |
| 13 | 600 W/m ² + 0.375 m ² | 15.24 | 17.80 |
| 14 | 800 W/m ² + 0.375 m ² | 21.29 | 21.18 |
| 15 | 1000 W/m ² + 0.375 m ² | 17.06 | 21.27 |
| 16 | 200 W/m ² + 0.500 m ² | -10.95 | -10.95 |
| 17 | 400 W/m ² + 0.500 m ² | -10.88 | -10.89 |
| 18 | 600 W/m ² + 0.500 m ² | 14.16 | -10.85 |
| 19 | 800 W/m ² + 0.500 m ² | 15.06 | 20.52 |
| 20 | 1000 W/m ² + 0.500 m ² | 16.21 | 20.84 |

As shown in the first part of the study, again, the cavity width of the facade cavity had a minimal effect on the achieved air temperatures in the cavity or at the outlet.

When combining the lowest solar radiation intensity of 200 W/m² with the largest exhaust area of 0.500 m², the average temperature of the exhaust air is almost identical to the outside air temperature of -10.8 °C. On the contrary, with a solar radiation intensity of 1000 W/m² and a smallest exhaust area of 0.125 m², this temperature is up to almost 32-36 K higher and reaches +20.8 °C in the case of the cavity width of 1200 mm, and +16.2 °C in the case of the cavity width of 600 mm, which is almost 5.5 K less.

A deeper analysis of the results revealed that the air temperature rises in the facade cavity, due to solar radiation, accompanied by the classic

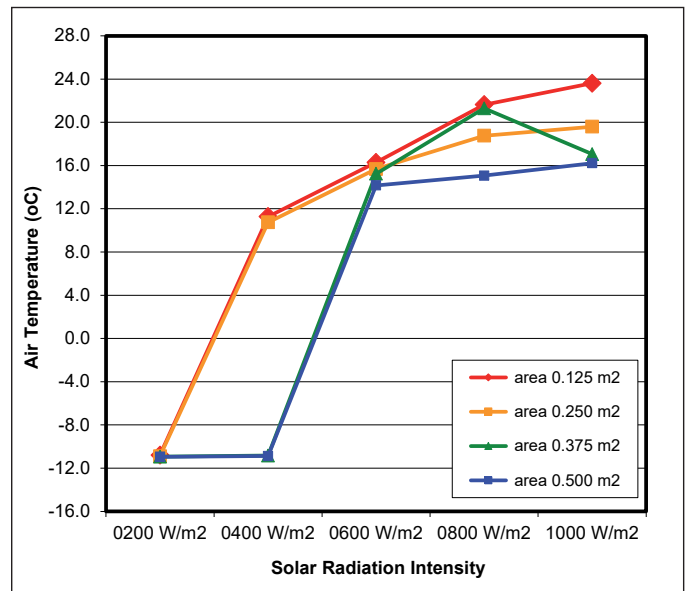


Figure 5 The air temperature at the outlet from the facade cavity, width 600 mm.

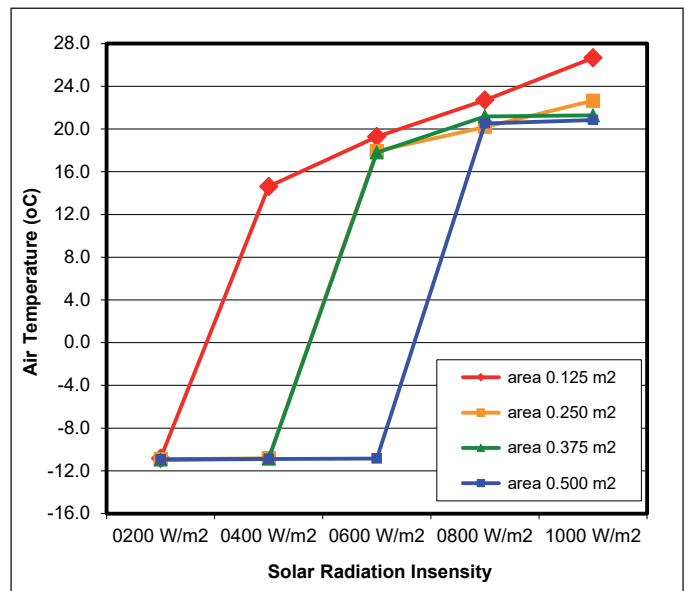


Figure 6 The air temperature at the outlet from the facade cavity, width 1200 mm

chimney effect – causing the hot air in the cavity to rise, which occurs only under certain boundary and geometric conditions. It can also be clearly seen in Fig. 5 and 6.

With a facade cavity width of 600 mm and a minimum solar radiation intensity of 200 W/m², the cold exterior air at all four exhaust surfaces pushes out any chimney effect, preventing the air from flowing outwards, and this cold air falls to the bottom of the entire cavity. At a solar radiation intensity of 400 W/m², this phenomenon is repeated, but smaller openings of 0.125 and 0.250 m² can already initiate the chimney effect and, thus, there is good air flow. At an intensity of 600 W/m² and more, but without any difference in the area, the DSF ensures the air flow in the cavity rises, and it also considerably overheats. It works almost identically, even with a facade cavity width of 1200 mm, with the only difference that the air enters the exhaust and falls in the cavity even with a radiation of 600 W/m² in combination with the largest opening of 0.500 m².

The change in the direction of air flow, thus, represents a significant change in the air temperatures in the order of 20-25 K at the exhaust

Table 4 Average air temperature in the facade cavity

| No. | variant | 0600 mm | 1200 mm |
|-----|--|---------|---------|
| 01 | 200 W/m ² + 0.125 m ² | -5.34 | -5.97 |
| 02 | 400 W/m ² + 0.125 m ² | 3.07 | 5.30 |
| 03 | 600 W/m ² + 0.125 m ² | 4.84 | 7.12 |
| 04 | 800 W/m ² + 0.125 m ² | 6.12 | 8.56 |
| 05 | 1000 W/m ² + 0.125 m ² | 8.50 | 10.50 |
| 06 | 200 W/m ² + 0.250 m ² | -8.34 | -7.93 |
| 07 | 400 W/m ² + 0.250 m ² | 2.57 | -4.15 |
| 08 | 600 W/m ² + 0.250 m ² | 4.42 | 6.09 |
| 09 | 800 W/m ² + 0.250 m ² | 5.86 | 6.85 |
| 10 | 1000 W/m ² + 0.250 m ² | 6.05 | 7.86 |
| 11 | 200 W/m ² + 0.375 m ² | -9.33 | -8.28 |
| 12 | 400 W/m ² + 0.375 m ² | -4.15 | -6.21 |
| 13 | 600 W/m ² + 0.375 m ² | 4.00 | 5.91 |
| 14 | 800 W/m ² + 0.375 m ² | 5.83 | 6.87 |
| 15 | 1000 W/m ² + 0.375 m ² | 4.25 | 7.02 |
| 16 | 200 W/m ² + 0.500 m ² | -8.98 | -9.25 |
| 17 | 400 W/m ² + 0.500 m ² | -7.34 | -8.05 |
| 18 | 600 W/m ² + 0.500 m ² | 3.59 | -4.50 |
| 19 | 800 W/m ² + 0.500 m ² | 3.45 | 6.48 |
| 20 | 1000 W/m ² + 0.500 m ² | 3.76 | 6.67 |

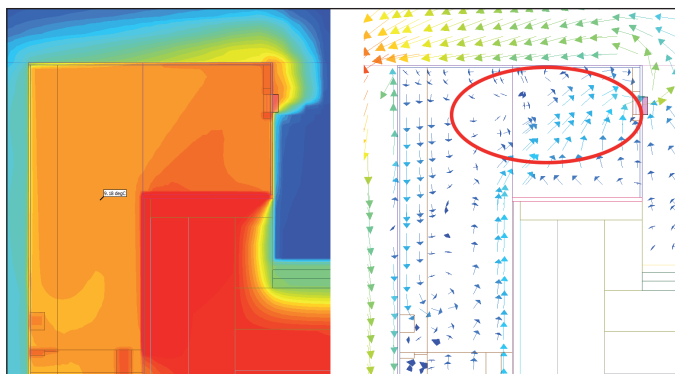


Figure 7 Air temperature and flow vectors for the variant: cavity width 600 mm + solar radiation 400 W/m² + area 0.125 m²

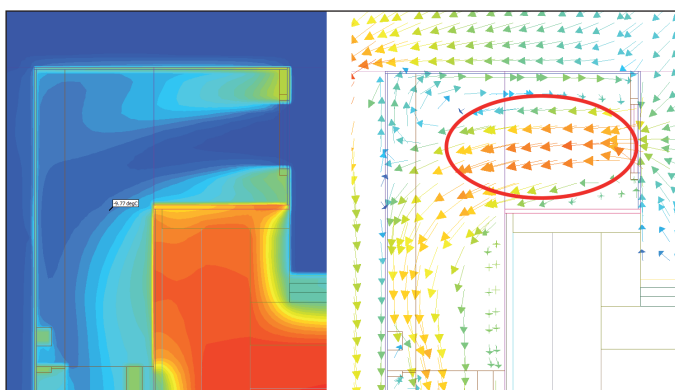


Figure 8 Air temperature and flow vectors for the variant: cavity width 600 mm + solar radiation 400 W/m² + area 0.500 m²

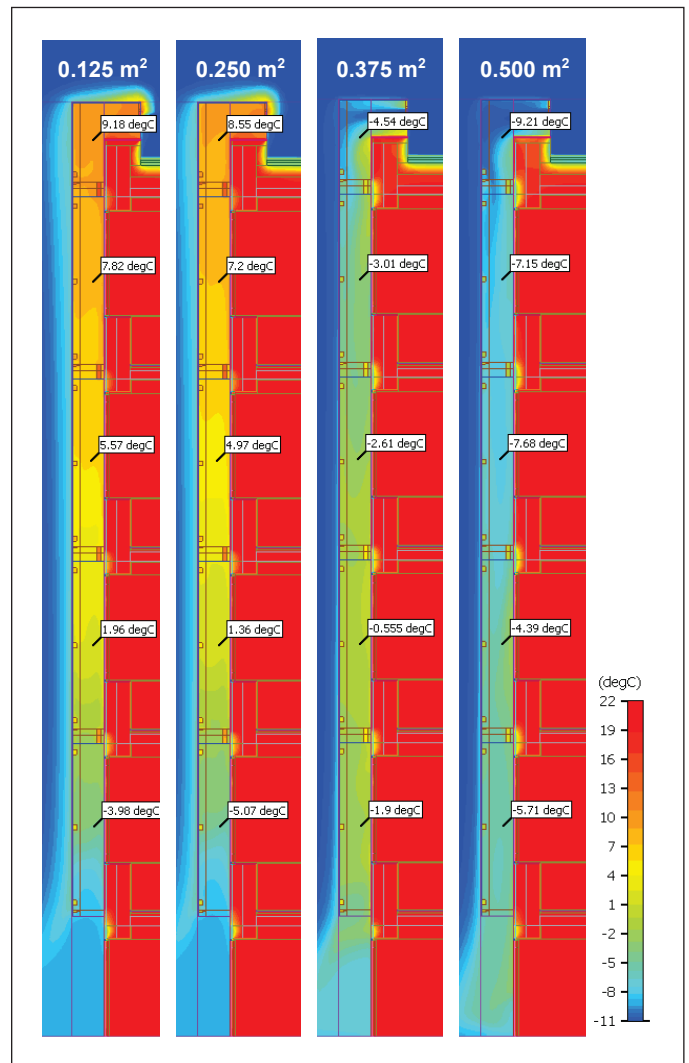


Figure 9 Air temperature in the facade cavity – cavity width 600 mm, radiation 400 W/m², exhaust opening 0.125, 0.250, 0.375 and 0.500 m² (cross section)

and 8-12 K at the level of the average temperature in the facade cavity and only with a change in the intensity of solar radiation by 200 W/m².

The phenomenon described above is depicted even more in Fig. 7 and 8, which documents the limit variants of the solar radiation intensity of 400 W/m² at the area of 0.125 m² and 0.500 m², with a facade cavity width of 600 mm. The classic chimney effect (Fig. 7) and the vice versa, so-called reverse effect, occurred (Fig. 8), i.e., the cold air inlet and its suction through the outlet (expressed through the air temperature and flow vectors). These phenomena can also be observed in Fig. 9, where the ambient air temperatures are expressed for the specific boundary condition of 400 W/m².

For a simple comparison with the first part of the analysis - realised in the form of forced ventilation (Tab. 4), which presents the average air temperatures in the facade cavity, the results are significantly higher in this case, i.e., the air flows achieved by the free opening are significantly lower than expected in the version with forced ventilation - using a heat pump.

CONCLUSION

The presented energy simulation study with 48 variants of the DSF configurations with forced ventilation and 40 variants of the DSF configurations with natural ventilation proved:

- The minimal effect of the width of the facade cavity on the air temperature conditions within the cavity,
- with a total visual area of approximately 63.0 m², it is possible to achieve a gross instantaneous energy output of approximately 19.5 kW,
- a significant increase in the average temperatures of the facade cavity up to 0 °C in forced ventilation and +10.5 °C in natural ventilation, with an increasing solar radiation intensity at the lowest flow,
- the phenomenon called the return effect, where the cold air falls back into the facade cavity (and results in its significant cooling) through the upper opening, approximately to the level of solar radiation intensity 400 W/m².

It is necessary to design a DSF with regard to its various specifics, the above-mentioned dependencies and real efficiencies in various boundary conditions, such as solar radiation, air flow - forced or natural, so that, in addition to the architectural aspect, the energy part also plays a significant role.

Acknowledgment: This work was supported by the Slovak Research and Development Agency under contract no. APVV-18-0174, by the Scientific Grant Agency of the Ministry of Education, Science, Research and Sport of the Slovak Republic under research project VEGA 1/0050/18, and by the project GA 20-00630S "Climate responsive components integrated in energy and environmentally efficient building envelope" supported by the Czech Science Foundation in Czechia.

Contact: e-mail: peter.buday@stuba.sk

References

- [1] GHAFARIANHOSEINI A. Ghaffarianhoseini Amirhosein Exploring the advantages and challenges of double-skin façades (DSFs). *Renewable and Sustainable Energy Reviews*. 2016, Vol. 60, 1052-1065.
- [2] WOO Lee S., PARK J. S. Evaluating thermal performance of double-skin facade using response factor. *Energy and Buildings*. 2020, Vol. 209.
- [3] ALBERTO A., RAMOS N. M. M., ALMEIDA R. M. S. F. Parametric study of double-skin facades performance in mild climate countries. *Journal of Building Engineering*. 2017, Vol. 12, 87 – 98.
- [4] YOON Y. B., SEO B., KOH B. B., CHO S. Performance analysis of a double-skin facade system installed at different floor levels of high-rise apartment building. *Journal of Building Engineering*. 2019, Vol. 26.
- [5] SANCHEZ E., ROLANDO A., SANT R., AYUSO L. Influence of natural ventilation due to buoyancy and heat transfer in the energy efficiency of a double skin facade building. *Energy for Sustainable Development*. 2016, Vol. 33, 139 – 148.
- [6] DA SILVA F. M., GOMES M. G., RODRIGUES A. M. Measuring and estimating airflow in naturally ventilated double skin facades. *Building and Environment*. 2015, Vol. 87, 292 – 301.
- [7] SANCHEZ E., ROLANDO A., SANT R., AYUSO L. Determination of the optimal thickness of vertical air channels in double-skin solar façades. *Energy Procedia*. 2019, Vol. 158, 1255 – 1260.
- [8] YANG H., ZHOU Y., JIN F., ZHAN X. Thermal Environment Dynamic Simulation of Double Skin Façade with Middle Shading Device in Summer. *Procedia Engineering*. 2016, Vol. 146, 251 – 256.
- [9] STN 73 0540-2. Thermal protection of buildings. Thermal performance of buildings and components. Part 2: Functional requirements. April 2019.
- [10] FloVENT® 3D Computational Fluid Dynamics Software [software]. Available from: <https://www.mentor.com>

Symbols

| | |
|-----------|--|
| W | cavity width [mm] |
| R_E | solar reflectance [-] |
| A_E | solar absorptance [-] |
| T_E | solar transmittance [-] |
| U_g | thermal transmittance of Glazing [W·m ⁻² ·K ⁻¹] |
| I_{sol} | solar radiation intensity [W·m ⁻²] |
| θ | air temperature [°C] |
| Q | immediate façade performance [kW] |
| V | air flow [m ³ ·h ⁻¹] |
| A | area [m ²] |